Am J Physiol Cell Physiol 311: C190–C200, 2016.
First published June 8, 2016; doi:10.1152/ajpcell.00066.2016.

CALL FOR PAPERS | *Regulation of Cell Signaling Pathways*

Mitochondrial maintenance via autophagy contributes to functional skeletal muscle regeneration and remodeling

Anna S. Nichenko,[1]* W. Michael Southern,[1]* Mark Atuan,[1,2] Junna Luan,[3] Kristen B. Peissig,[3] Steven J. Foltz,[3] Aaron M. Beedle,[3] Gordon L. Warren,[4] and Jarrod A. Call[1,2]

[1]*Department of Kinesiology, University of Georgia, Athens, Georgia;* [2]*Regenerative Bioscience Center, University of Georgia, Athens, Georgia;* [3]*Department of Pharmaceutical and Biomedical Sciences, University of Georgia, Athens, Georgia; and* [4]*Department of Physical Therapy, Byrdine F. Lewis School of Nursing and Health Professions, Georgia State University, Atlanta, Georgia*

Submitted 26 February 2016; accepted in final form 1 June 2016

Nichenko AS, Southern WM, Atuan M, Luan J, Peissig KB, Foltz SJ, Beedle AM, Warren GL, Call JA. Mitochondrial maintenance via autophagy contributes to functional skeletal muscle regeneration and remodeling. *Am J Physiol Cell Physiol* 311: C190–C200, 2016. First published June 8, 2016; doi:10.1152/ajpcell.00066.2016.—The primary objective of this study was to determine whether alterations in mitochondria affect recovery of skeletal muscle strength and mitochondrial enzyme activity following myotoxic injury. 3-Methyladenine (3-MA) was administered daily (15 mg/kg) to blunt autophagy, and the creatine analog guanidionpropionic acid (β-GPA) was administered daily (1% in chow) to enhance oxidative capacity. Male C57BL/6 mice were randomly assigned to nontreatment (Con, $n = 6$), 3-MA-treated ($n = 6$), and β-GPA-treated ($n = 8$) groups for 10 wk. Mice were euthanized at 14 days after myotoxic injury for assessment of mitochondrial remodeling during regeneration and its association with the recovery of muscle strength. Expression of several autophagy-related proteins, e.g., phosphorylated Ulk1 (~2- to 4-fold, $P < 0.049$) was greater in injured than uninjured muscles, indicating a relationship between muscle regeneration/remodeling and autophagy. By 14 days postinjury, recovery of muscle strength (18% less, $P = 0.03$) and mitochondrial enzyme (e.g., citrate synthase) activity (22% less, $P = 0.049$) were significantly lower in 3-MA-treated than Con mice, suggesting that the autophagy process plays an important role during muscle regeneration. In contrast, muscle regeneration was nearly complete in β-GPA-treated mice, i.e., muscle strength recovered to 93% of baseline vs. 78% for Con mice. Remarkably, 14 days allowed sufficient time for a near-complete recovery of mitochondrial function in β-GPA-treated mice (e.g., no difference in citrate synthase activity between injured and uninjured, $P = 0.49$), indicating a robust mitochondrial remodeling process during muscle regeneration. In conclusion, autophagy is likely activated following muscle injury and appears to play an important role in functional muscle regeneration.

mitophagy; Unc-51-like autophagy-activating kinase 1; torque

MUSCLE REPAIR occurs in four main phases: degeneration, inflammation, regeneration, and remodeling (15). Satellite cells activated during the early phases of muscle repair largely contribute to muscle regeneration, primarily by providing nuclei. The latter remodeling phase plays an important role in final restoration of contractile, structural, and metabolic organelles critical to complete recovery of muscle function. Emerging evidence indicates a transition in metabolic demand during muscle regeneration and remodeling that may signify an important role of the mitochondria in muscle repair (25). Importantly, myoblast differentiation is terminated if mitochondrial DNA (mtDNA) replication is impaired in vitro (12). Additionally, genes associated with mitochondrial biogenesis are upregulated 3–10 days after injury in vivo (28). Therefore, the energy demands of muscle regeneration may rely in part on the contribution of oxidative phosphorylation from the mitochondria. There is evidence of mitochondrial damage after muscle injury (9, 28), and the cellular mechanisms responsible for removal and replacement of those damaged mitochondria are not completely known.

The potential impact of impaired mitochondrial maintenance on skeletal muscle recovery is worth considering, particularly if an accumulation of dysfunctional mitochondria after several bouts of muscle injury could negatively affect muscle function. In support of this idea, muscle function was improved following genetically induced mitochondrial biogenesis in a mouse model of Duchenne muscular dystrophy that is characterized by perpetual muscle injury and regeneration (*mdx* mouse) (27). Additionally, stimulation of autophagy (a cellular process essential for degradation of dysfunctional and/or damaged organelles) in the *mdx* mouse decreased the presence of dysfunctional mitochondria and was associated with an improvement in muscle function (24). These studies suggest that manipulation of muscle mitochondria can impact muscle function and support a model in which mitochondrial remodeling after injury may utilize autophagy to remove damaged mitochondria. Accordingly, impaired or insufficient autophagy could lead to an accumulation of dysfunctional mitochondria, which could adversely affect a muscle's function if the muscle were to undergo repeated bouts of injury. The role of autophagy during muscle regeneration is unclear, but autophagy is critical for maintaining skeletal muscle mass in young and aged mice (19, 26); therefore, autophagy may contribute to a muscle's health in many ways. Elucidation of the relationship between autophagy and muscle repair could provide therapeutic targets to enhance muscle regeneration.

The primary objective of this study was to determine the extent to which alterations in mitochondria affect functional

* A. S. Nichenko and W. M. Southern contributed equally to this work.
Address for reprint requests and other correspondence: J. A. Call, 330 River Rd., Ramsey Center, Dept. of Kinesiology, Univ. of Georgia, Athens, GA 30602 (e-mail: call@uga.edu).

muscle regeneration and the remodeling of mitochondria after injury. A broad-range autophagy inhibitor [3-methyladenine (3-MA)] and a creatine analog [guanidinopropionic acid (β-GPA)] were used to impair and enhance, respectively, the mitochondria in skeletal muscle. We hypothesized that muscle regeneration would be associated with an autophagy response and that manipulation of the mitochondria would affect functional muscle and mitochondrial regeneration.

MATERIALS AND METHODS

Experimental design. Eight-week-old male C57BL/6J mice (Jackson Laboratories) were housed at 20–23°C on a 12:12-h light-dark cycle, with food and water provided ad libitum. At 9 wk of age, mice were randomized to control (Con, $n = 6$), 3-MA-treated ($n = 6$), and β-GPA-treated ($n = 8$) groups. To detect a 15% difference in recovery of muscle strength at 14 days postinjury with the assumption of a power of 0.7 and an α-level of 0.05, it was determined, on the basis of our previous physiological muscle contractility measurements for control C57BL/6J mice, that sample sizes of at least five mice per group were necessary. At least one additional mouse per group was included to account for experimental losses.

To determine if 3-MA or β-GPA affected muscle function in the absence of injury, contractile functions (i.e., peak isometric strength and fatigue) were analyzed for the ankle dorsiflexor muscles (tibialis anterior, extensor digitorum longus, and extensor hallucis longus) after 8 wk of treatment. Immediately following contractile assessment of the dorsiflexor muscles, the tibialis anterior and gastrocnemius muscles were injected with cardiotoxin to induce injury. The rationale for injuring the gastrocnemius muscles was to have sufficient tissue for biochemical assessment at 14 days postinjury. Muscle strength was assessed 1 min after cardiotoxin injection and used as the immediate-postinjury time point. Peak isometric strength was assessed again at 14 days postinjury. This time point was selected because it allows sufficient time for satellite cell activation and differentiation and because previous reports have identified this as a time when mitochondrial remodeling postinjury is ongoing (9, 28). The tibialis anterior and gastrocnemius muscles were harvested immediately after the 14-day postinjury contractile assessment. The gastrocnemius was finely minced and separated for mitochondrial enzyme activity assessment and immunoblot analysis. Each tibialis anterior muscle was preserved for histology. All procedures were approved by the Institutional Animal Care and Use Committee at the University of Georgia.

Treatments and myotoxic injury. 3-MA inhibits phosphatidylinositol and phagosome formation and is classified as a broad-range autophagy inhibitor. 3-MA-treated mice received daily injections of 3-MA (15 mg/kg sc). β-GPA is a creatine analog that reduces phosphocreatine availability within skeletal muscle and leads to greater signaling for mitochondrial biogenesis (22). β-GPA was administered via rodent chow (Teklad) in a 1% proportion. All mice received chow ad libitum for the duration of the study. Mice were rendered unconscious using isoflurane (1.5%) and subjected to muscle injury, as previously described (14). Briefly, 40 μl of cardiotoxin (*Naja kaouthia*, 0.071 mg/ml; catalog no. C9759, Sigma-Aldrich) were injected into the left tibialis anterior muscles. The medial and lateral gastrocnemius muscles also received 40-μl injections, and a third 40-μl injection was delivered between the two portions of the gastrocnemius muscle.

In vivo assessment of muscle contractility. In vivo peak isometric torque of the dorsiflexor muscles was assessed as previously described (6). Briefly, anesthesia was induced using an induction chamber and 5% isoflurane in oxygen. Anesthesia was maintained using 1–2% isoflurane. The left hindlimb was depilated and aseptically prepared, and the foot was placed in a footplate attached to a servomotor (model 300C-LR, Aurora Scientific, Aurora, ON, Canada). Pt-Ir needle electrodes (catalog no. E2-12, Grass Technologies, West Warwick, RI) were inserted percutaneously on either side of the common peroneal nerve. The ankle joint was adjusted to a 90° angle. Peak isometric torque was achieved by varying the position of the electrodes and the current delivered to the peroneal nerve using a 0.1-ms square-wave pulse at a frequency of 200 Hz. During functional testing, the testing platform was heated to 37°C to maintain the animal's body temperature. Torque as a function of stimulation frequency was then measured during nine isometric contractions at varying stimulation frequencies (5, 10, 20, 40, 60, 80, 100, 150, and 200 Hz). Finally, muscle fatigability was assessed by 120 isometric contractions, one elicited every second using a 300-ms, 60-Hz stimulation. To account for differences in body size among mice, torque (mN·m) was normalized by body mass (kg).

Mitochondrial enzyme activity assays. Gastrocnemius muscles were homogenized in 33 mM phosphate buffer (pH 7.4) at a muscle-to-buffer ratio of 1:20 using a glass tissue grinder on ice. Protein concentration of each homogenate was measured using the bicinchoninic acid protein assay (Thermo Fisher Scientific). Citrate synthase (CS), β-hydroxy acyl-CoA dehydrogenase (β-HAD), and cytochrome *c* oxidase (complex IV) activities were determined as previously described (5, 16). Isocitrate dehydrogenase (IDH) activity was measured by the reduction of NAD^+ at an absorbance of 340 nm (37°C). This was achieved by addition of 5 μl of muscle homogenate to 170 μl of assay buffer (pH 8.5, 0.2 M Tris and 1 mM $MgCl_2$), 10 μl of NAD^+ (3.2 mM; catalog no. N0632, Sigma), and 10 μl of DL-isocitrate (4.6 mM; catalog no. I1252, Sigma). Complex I activity was measured by the reduction of cytochrome *c* at an absorbance of 550 nm (30°C). This was achieved by addition of 2.5 μl of muscle homogenate to 90 μl of oxidized cytochrome *c* (0.1 mM; catalog no. C2506, Sigma) and 90 μl of NADH (1 mM; catalog no. N8129, Sigma). In separate wells with identical conditions, the same sample was analyzed with the addition of rotenone (0.1 mM) to block complex I electron transport. The difference between the activities represents complex I activity (11). Complex II activity was measured by the reduction of cytochrome *c* at an absorbance of 550 nm (30°C). This was accomplished by addition of 15 μl of muscle homogenate to 100 μl of 0.5 M sodium succinate in a 3-ml cuvette for 1 min, followed by the addition of 100 μl of sodium cyanide (0.01 M) and 2.8 ml of cytochrome *c* buffer (22.7 mM). Enzyme activities were run in triplicate and are normalized to total protein content.

Immunoblot analysis. For protein analysis, the gastrocnemius muscle was immediately homogenized with glass homogenizers in protein loading buffer and loaded on a gel for SDS-PAGE and immunoblotting, as previously described (4). The following antibodies (Cell Signaling, Danvers, MA) were used to probe proteins transferred to polyvinylidene difluoride membranes: cytochrome *c* oxidase IV (COX IV, 1:1,000 dilution), cytochrome *c* (1:1,000 dilution), microtubule-associated protein 1B-light chain 3 (LC3B, 1:1,000 dilution), p62/SQSTM1 (1:1,000 dilution), Unc-51-like autophagy-activating kinase 1 (Ulk1, 1:1,000 dilution), phosphorylated (Ser^{555}) Ulk1 (1:1,000 dilution), Bnip3 (1:1,000 dilution), dynamin-related protein 1 (Drp1, 1:1,000 dilution), 5′-AMP-activated protein kinase (AMPK)-α (1:1,000 dilution), phosphorylated (Thr^{172}) AMPKα (1:1,000 dilution), and β-actin (1:5,000 dilution). Membranes were analyzed and quantified using Image Lab software (Bio-Rad Laboratories, Hercules, CA).

Real-time PCR. The ratio of mtDNA to nuclear DNA (nDNA) was determined by quantitative real-time PCR. Primer sequences for mitochondrial *12S* ribosomal DNA included 5′-ACCGCGGTCATACGATTAAC-3′ (forward) and 5′-CCCAGTTTGGGTCTTAGCTG-3′ (reverse). Mitochondrial *12S* ribosomal DNA was analyzed relative to three reference genes: *18S* nDNA [5′-TTGATTAAGTCCCTGCCCTTTGT-3′ (forward) and 5′-CGATCCGAGGGCCTAACTA-3′ (reverse)], heat shock protein 90 (*Hsp90ab1*; Mm00833431_g1, Fisher Scientific), and hypoxanthine-guanosine phosphoribosyltransferase (*Hprt*; Mm03024075_m1, Fisher Scientific).

Histological and immunofluorescence assessments. The tibialis anterior and extensor digitorum longus muscles were dissected together and frozen in 2-methylbutane cooled to −160°C in a liquid nitrogen bath. Sections (7 μm thick) were cut by cryostat (catalog no. HM550, Thermo Scientific) and mounted on microscope slides. Tissues were stained for immunofluorescence according to standard protocols (2, 10). Briefly, slides were moistened with phosphate-buffered saline (PBS) and blocked with 5% donkey serum (Jackson ImmunoResearch) in PBS. Primary antibody was diluted in blocking solution and incubated overnight at 4°C. Slides were washed three times with PBS, incubated with appropriate secondary antibodies and 4′,6-diamidino-2-phenylindole (1:10,000 dilution; Sigma) for 30 min at room temperature, washed three times, and mounted with PermaFluor mounting medium (Thermo Scientific). Muscle sections were imaged using an inverted epifluorescence microscope (model X71, Olympus) and cellSens software (Olympus). Entire muscle cross sections were captured by a series of overlapping ×20 images. Individual fluorescence images were merged and compiled to generate the complete muscle map in Photoshop (Adobe). Total fibers, number of antibody-positive fibers, and fiber areas were analyzed using manual tag or area measurements in Image-Pro Express (Media Cybernetics). For indirect immunofluorescence, primary antibodies were used to detect myosin heavy chain type 1, myosin heavy chain type 2a, and embryonic myosin heavy chain fiber types (eMHC, 1:30–1:40 dilution; catalog nos. BA-D5, SC-71, and F1.652, respectively, Developmental Studies Hybridoma Bank), in blood vessels (1:50 dilution; CD31, BD Pharmingen), and sarcolemmal or extracellular matrix markers [α-dystroglycan (aDGct, catalog no. 5-2 or 45-4, Developmental Studies Hybridoma Bank), 1:25 dilution (10) and β-dystroglycan (catalog no. MANDAG2 7D11, Developmental Studies Hybridoma Bank), 1:40 dilution] or collagen VI (catalog no. 70R-CR009x, Fitzgerald Industries; 1:1,000 dilution) was used to identify individual fibers. For p62 analysis by immunofluorescence, slides were fixed in precooled methanol for 15 min at −20°C. After they were washed five times with PBS, slides were blocked for 30 min at room temperature in 5% donkey serum (Jackson ImmunoResearch), 2% BSA (Sigma), and 0.1% Triton-X 100 (Sigma) in PBS. Slides were incubated overnight at 4°C in anti-p62 (Sigma) and anti-perlecan (heparin sulfate proteoglycan; Millipore), both at 1:100 dilution. All slides were washed three times with PBS, incubated with anti-rabbit Alexa Fluor 546 (1:500 dilution), anti-rat Alexa Fluor 488 (1:500 dilution), and 4′,6-diamidino-2-phenylindole (1:10,000 dilution) for 30 min at room temperature, washed three times, and mounted with PermaFluor (Thermo Fisher). Images were collected with the ×40 objective using an inverted epifluorescence microscope (model IX71, Olympus).

Cell culture. Mouse muscle myoblast C2C12 cells (CRL-1772, American Type Culture Collection) were expanded, according to standard protocols, in myoblast medium: Dulbecco's modified Eagle's medium and 4.5 g/l glucose (DMEM; Corning), supplemented with 15% FBS (Atlanta Biologicals), 1:100-diluted glutaMAX (Gibco), and 1:100-diluted antibiotic-antimycotic solution (Corning). C2C12 cells were plated in myoblast medium at 120,000 cells/well in six-well tissue culture-treated plates. At ~24 h after the cells were plated, myoblast medium was removed and replaced with saline vehicle (2 wells), 1 mM 3-MA (2 wells), or 1 mM β-GPA (2 wells) in differentiation medium (DMEM, 2% FBS, 1:100-diluted glutaMAX, and 1:100-diluted antibiotic-antimycotic). Medium with saline, 3-MA, or β-GPA was refreshed every 48 h. After 6 days of differentiation, one drop of the nuclear stain NucBlue (Thermo Fisher) was added to each well, and the samples were incubated for 30 min at room temperature. Phase-contrast (gray-scale) and blue-fluorescence (NucBlue) images were collected from three different locations from each well using an epifluorescence microscope (model IX71, Olympus) with cellSens software. Images were analyzed for the number of cells with myotube-like morphology (elongated, with or without multiple nuclei) for each ×10 field and averaged across all images per well.

Statistical analysis. Values are means ± SD. Two-way repeated-measures ANOVA was used to analyze the data. The between-subject factor was treatment group (Con vs. 3-MA vs. β-GPA) and the repeated-measure factor varied between time point (pre- vs. postinjury) and limb (uninjured vs. injured). Data were required to pass normality (Shapiro-Wilk test) and equal variance (Brown-Forsythe *F*-test) tests before they were subjected to the repeated-measures ANOVA. Differences among groups are reported only where significant interactions were observed and subsequently tested with Tukey's post hoc test using JMP statistical software (SAS, Cary, NC). Group main effects are reported where significant interactions were not observed. An α-level of 0.05 was used for all analyses.

RESULTS

Effect of treatments on body mass and uninjured muscle contractility. To determine the impact of treatment on uninjured muscle, dorsiflexor contractility was assessed immediately prior to muscle injury, i.e., 8 wk after initiation of 3-MA, β-GPA, or Con treatment. Autophagy inhibition with 3-MA had no effect on body mass, muscle strength, or muscle fatigue after 8 wk of treatment (Fig. 1). β-GPA-treated mice, however, did not gain body mass during the treatment period and generated torques ~20% less than Con and 3-MA-treated mice (Fig. 1, *A* and *B*). β-GPA-treated mice subjected to a metabolically challenging contractile test had greater fatigue resistance than Con mice (contraction number 100 to 150, $P \leq 0.045$) and 3-MA-treated mice (contraction number 90 to 150, $P \leq 0.041$; Fig. 1*C*). By the end of the fatigue protocol, β-GPA-treated mice were generating 40%, while Con and 3-MA-treated mice were generating only 29%, of the peak isometric torque measured before the fatigue protocol (Fig. 1*C*). These data suggest that the 3-MA regimen did not impact skeletal muscle contractility, while β-GPA resulted in a weaker muscle but was effective in increasing dorsiflexor muscle fatigue resistance.

Effect of treatments on recovery of contractile function following injury. After 8 wk of 3-MA or β-GPA treatment, a myotoxic injury model was used to damage skeletal muscle and initiate muscle regeneration in the tibialis anterior and gastrocnemius muscles. There was no difference among groups in peak isometric torque of the dorsiflexors immediately following cardiotoxin injection ($P = 0.95$), indicating that muscle damage was equivalent across groups. Peak isometric torque of the dorsiflexors was again tested 14 days postinjury to assess the effectiveness of muscle regeneration in the three groups. Muscles were significantly weaker in 3-MA-treated than Con and β-GPA-treated mice at 14 days postinjury (Fig. 2*A*). In fact, muscle strength in 3-MA-treated mice had recovered to only 58% of preinjury strength by 14 days postinjury, which is in stark contrast to Con (78%) and β-GPA-treated (93%) mice (Fig. 2*B*). This suggests that a broad-acting autophagy inhibitor can negatively impact functional muscle regeneration.

Effect of treatments on uninjured and injured muscle mitochondrial enzyme activity following injury. To assess functional regeneration of mitochondria after injury, mitochondrial enzyme activity from injured and uninjured gastrocnemius muscles was assessed for critical enzymes in the tricarboxylic acid (Krebs) cycle, β-oxidation, and the electron transport chain. Significant interactions between treatment and limbs (injured vs. uninjured) were observed for CS ($P = 0.008$) and complex IV ($P = 0.045$) activities (Fig. 3, *A*–*F*). CS and

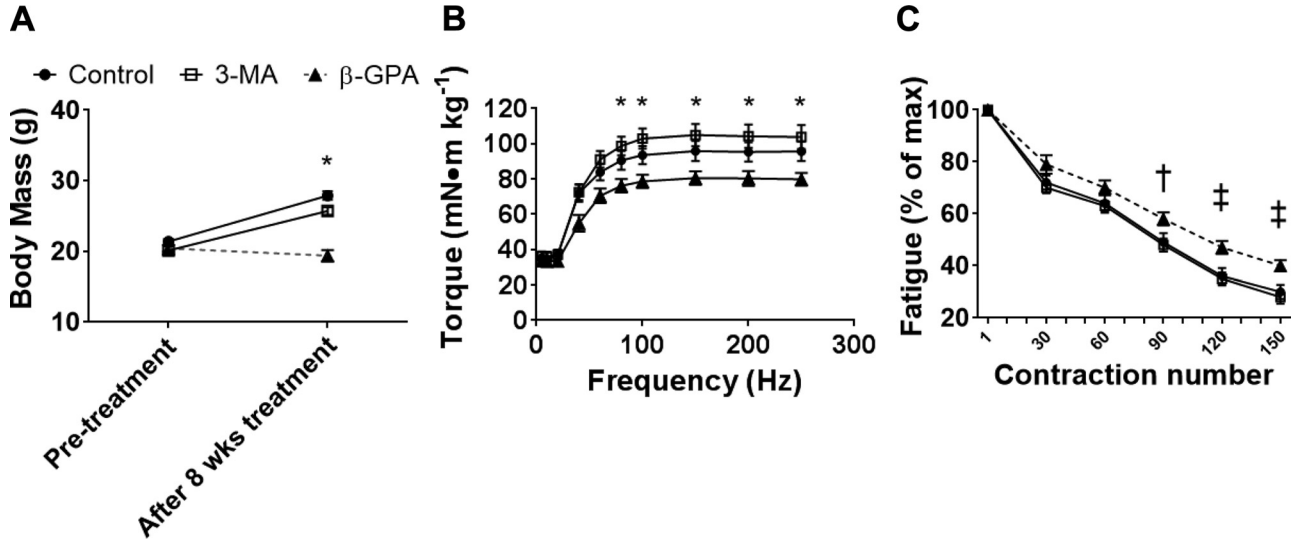

Fig. 1. Effect of 3-methyladenine (3-MA) and guanidinopropionic acid (β-GPA) treatments on body mass and uninjured muscle contractility. *A*: body mass at 9 wk of age (pretreatment) and after 8 wk of treatment. *B*: isometric torque as a function of stimulation frequency. *C*: torque loss from a fatiguing bout of contractions. Fatigue was calculated as a percentage of the greatest torque generated during the 120-contraction protocol. *β-GPA is significantly less than Con and 3-MA ($P < 0.05$). †β-GPA is significantly greater than 3-MA ($P < 0.05$). ‡β-GPA is significantly greater than control and 3-MA ($P < 0.05$).

complex IV activities were greater in uninjured muscle from β-GPA-treated mice than in uninjured muscle from Con and 3-MA-treated mice, supporting the ability of β-GPA to enhance oxidative capacity in uninjured skeletal muscle. Similarly, these enzyme activities were greater in the injured muscle from β-GPA-treated mice than in the injured muscle from Con and 3-MA-treated mice, suggesting that β-GPA may also enhance recovery of mitochondrial enzyme activity after injury. Only main effects were observed for β-HAD, IDH, complex I, and complex II activities, indicating that activities were lower in injured than uninjured muscles independent of treatment ($P \leq 0.034$). β-HAD and complex II activities were greater in β-GPA-treated and Con mice than 3-MA-treated mice independent of injury ($P \leq 0.035$), and IDH and complex I activities were greater in β-GPA- than 3-MA-treated mice independent of injury ($P \leq 0.048$; Fig. 3, *A–F*). To assess recovery of mitochondrial enzyme activity, the difference in muscle enzyme activity between injured and contralateral uninjured muscles for each mouse was calculated (shown as %deficit). For CS, IDH, β-HAD, and complex IV activities, there were no significant differences between uninjured and injured muscles after 14 days of recovery from Con ($P \geq 0.087$) and β-GPA treatment ($P \geq 0.074$), whereas the enzyme activity difference between injured and uninjured muscles for 3-MA-treated mice was 25–35% for all enzymes measured ($P \leq 0.042$). This analysis supports the idea that use of a broad-acting autophagy inhibitor during muscle regeneration significantly impairs the recovery of muscle mitochondrial enzyme activity.

Effect of treatments on uninjured and injured muscle mitochondrial protein content following injury. COX IV and cytochrome *c* protein content were assessed using immunoblotting for comparison with the enzyme activity results (Fig. 4, *A–C*). Independent of injury, COX IV protein expression was slightly, but significantly, greater in β-GPA-treated than Con and 3-MA-treated muscle (38%, $P < 0.001$; Fig. 4*B*). Independent of treatment, cytochrome *c* protein expression was ~52% greater in uninjured than injured muscle ($P = 0.031$; Fig. 4*C*). There was a trend ($P = 0.09$) for greater cytochrome *c* protein content in β-GPA-treated than Con and 3-MA-treated muscle. Importantly, there was no statistical difference in

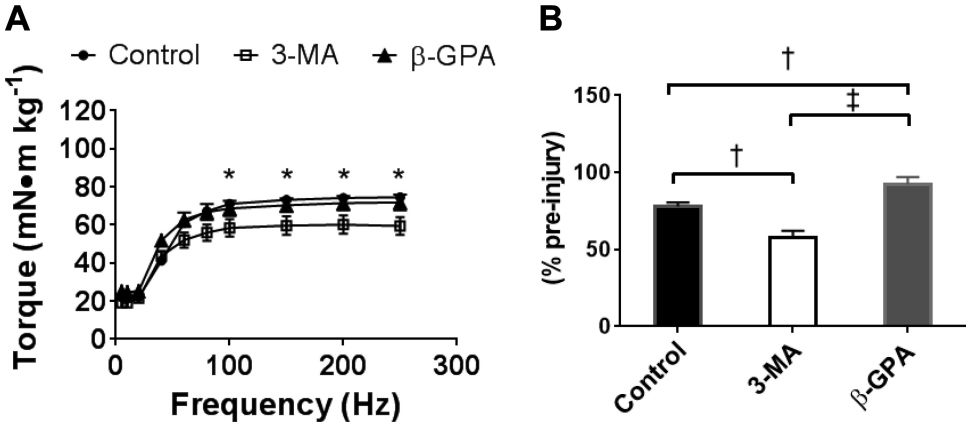

Fig. 2. Effect of 3-MA and β-GPA treatments on recovery of muscle contractility at 14 days postinjury. *A*: isometric torque as a function of stimulation frequency. *B*: percent recovery of peak isometric torque at 14 days postinjury. *3-MA is significantly less than Con and β-GPA ($P < 0.05$). †Significantly different from control ($P < 0.05$). ‡Significantly different from β-GPA ($P < 0.01$).

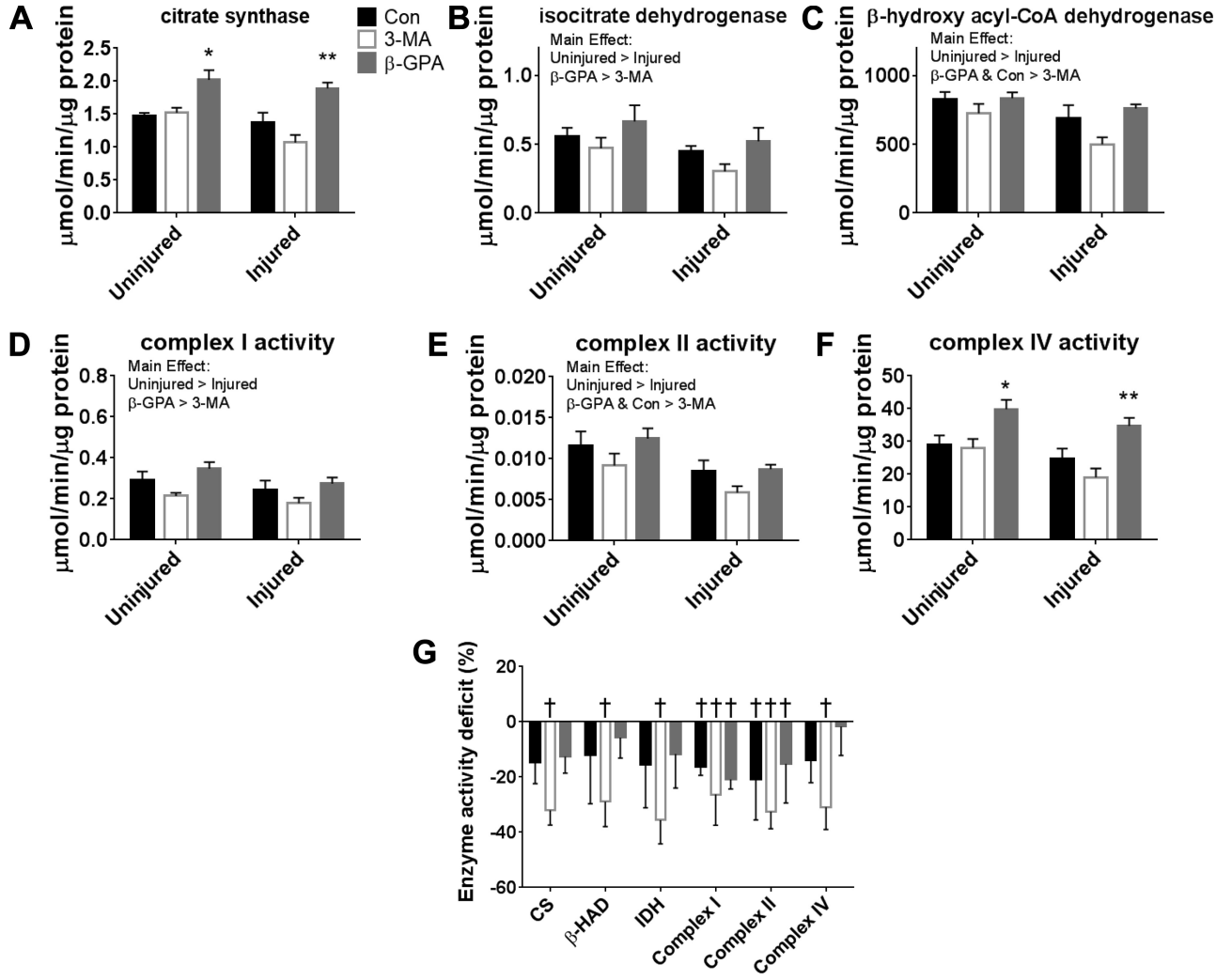

Fig. 3. Effect of treatments and muscle injury on mitochondrial enzyme activity. *A–F*: mitochondrial enzyme activity in uninjured and injured muscle from control (Con) and 3-MA- and β-GPA-treated mice. *G*: percent deficit of specific enzyme activity in injured gastrocnemius muscle 14 days postinjury compared with contralateral uninjured muscle. CS, citrate synthase; β-HAD, β-hydroxy acyl-CoA dehydrogenase; IDH, isocitrate dehydrogenase. *Significantly different from Con and 3-MA in uninjured muscle ($P < 0.05$). **Significantly different from Con and 3-MA in injured muscle. †Significantly different from contralateral uninjured muscle ($P < 0.05$).

mitochondrial protein contents between Con and 3-MA-treated mice.

Effect of treatments on uninjured and injured muscle mtDNA-to-nDNA ratio following injury. mtDNA content was assessed by quantitative PCR analysis of the mtDNA-to-nDNA ratio, which has been shown to correlate well with mitochondrial enzyme activity and reflect mitochondrial biogenesis (29, 34). There was a significant interaction between treatment and injury for the mtDNA-to-nDNA ratio ($P = 0.042$), and the mtDNA-to-nDNA ratio was greater in uninjured muscles from β-GPA-treated mice than in uninjured muscles from 3-MA-treated mice and injured muscles from β-GPA-treated, 3-MA-treated, and Con mice (Fig. 4*D*).

Effect of treatments on markers of muscle regeneration after injury. To determine if impaired muscle regeneration contributed to muscle strength and mitochondrial function recovery deficits in 3-MA-treated mice, histological assessment of regenerating tissue was quantified by the percentage of fibers that were centrally nucleated and the presence of fibers with eMHC. There was no difference in the number of centrally nucleated fibers among treatments (Fig. 5*A*). However, the percentage of eMHC-positive fibers was lower for injured muscles from β-GPA-treated than Con mice (Fig. 5*B*). At this time point, residual eMHC is very low; therefore, a physiological significance of this difference is unlikely. Lastly, the proportion of centrally nucleated muscle fibers with more than one central nuclei was analyzed. Notably, there were fewer fibers with multiple central nuclei in injured muscle from β-GPA-treated than Con mice (Fig. 5*C*).

To further investigate the impact of treatment on muscle regeneration, specifically to test if 3-MA negatively impacts myogenic differentiation and if β-GPA positively impacts myogenic differentiation, myotube formation was assessed by treating C2C12 cells with vehicle (Con), 3-MA, or β-GPA during a 6-day differentiation protocol. Successful myotube differentiation, as measured by elongated tubelike morphology, was observed under all treatment conditions (Fig. 5*D*), suggesting that treatment with 1 mM 3-MA does not impair

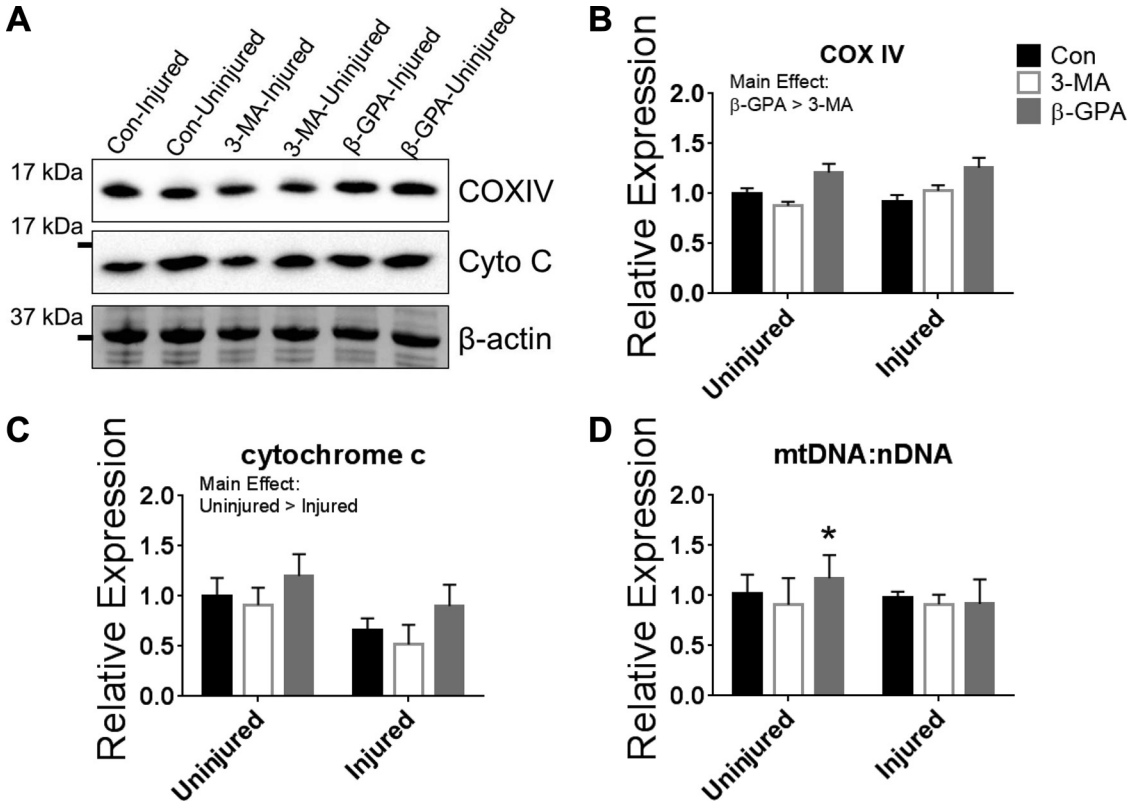

Fig. 4. Effect of treatments and muscle injury on markers of mitochondrial content. *A*: immunoblot images of cytochrome *c* oxidase IV (COX IV) and cytochrome *c* (Cyto *c*) in gastrocnemius muscle (30 μg of total protein). β-Actin was probed as loading control. *B* and *C*: quantitative and statistical analysis of data in *A* ($n = 6–8$/group). *D*: quantitative PCR ($n = 6–8$/group) for *12S* mitochondrial DNA (mtDNA) was assessed relative to nuclear DNA (nDNA) reference genes *18S*, hypoxanthine-guanosine phosphoribosyltransferase (*Hprt*), and heat shock protein 90 (*Hsp90ab1*) to determine the ratio of mtDNA to nDNA. *Statistically different from 3-MA-uninjured, Con-injured, 3-MA-injured, and β-GPA-injured.

myogenic differentiation. β-GPA-treated C2C12 cells (1 mM) had ~60% more myotube-like cells than Con and 3-MA-treated C2C12 cells after differentiation (Fig. 5*D*). The finding of fewer regenerated fibers with multiple central nuclei in β-GPA-treated mice following injury (Fig. 5*C*) and the enhanced differentiation in C2C12 cells in vivo suggest that β-GPA may enhance differentiation over proliferation after injury.

Effect of treatments on uninjured and injured muscle autophagy-related protein content following injury. To explore how autophagy may be contributing to the remodeling phase, we assessed the content of several autophagy-related proteins in injured and uninjured gastrocnemius muscle (Fig. 6*A*). A greater rate of initiation and resolution of autophagy (i.e., autophagy flux) was investigated by detection of LC3-II, the phosphatidylethanolamine-conjugated form of LC3-I that attaches to the autophagosome membrane, and p62, a cargo receptor for ubiquitinated substrates degraded by the autophagosome membranes (13, 20). Independent of treatment, total LC3, LC3-II, and p62 protein content was greater in injured than uninjured muscle ($P \leq 0.003$), suggesting enhanced autophagosome assembly during muscle regeneration. Additionally, muscle injury caused an accumulation of the autophagic marker p62, as intracellular p62 puncta were visible in injured muscle tissue sections from Con, 3-MA-treated, and β-GPA-treated mice compared with uninjured muscle sections (Fig. 6*B*). The extent to which these data signify autophagy flux during muscle regeneration is limited by the single-time-point study design (i.e., 14 days postinjury) but supports the premise that autophagy is induced even 14 days postinjury.

Total Ulk1 content (autophagy-related protein associated with degradation of mitochondria) was not different across treatment groups or injury at 14 days postinjury ($P = 0.455$; data not shown). However, there was a significant interaction of injury and treatment group for phosphorylated (activated) Ulk1 (Fig. 7; $P = 0.049$). In all treatment groups, activation of Ulk1 was greater (~2-fold) in injured than uninjured muscle. Also, basal activation of Ulk1 was greater in uninjured β-GPA- than uninjured 3-MA-treated muscle. Because Ulk1 activation is associated with mitophagy and the degradation of dysfunctional mitochondria, we further investigated the mitophagy protein Bnip3, which interacts with LC3 and plays a critical role in mitophagy (1, 35). Bnip3 protein content was significantly elevated in all injured muscle relative to uninjured contralateral muscle independent of treatment (Fig. 7; $P < 0.001$). Protein content for Drp1, a specialized protein that facilitates the removal of damaged or dysfunctional mitochondria from the mitochondrial network prior to mitophagy, was significantly greater in β-GPA-treated and Con than 3-MA-treated mice independent of injury ($P = 0.049$) and greater in injured than uninjured muscle independent of treatment (Fig. 7; $P = 0.023$). We observed no significant difference across groups in AMPK protein content (data not shown; $P = 0.877$), although phosphorylated AMPK was significantly greater in

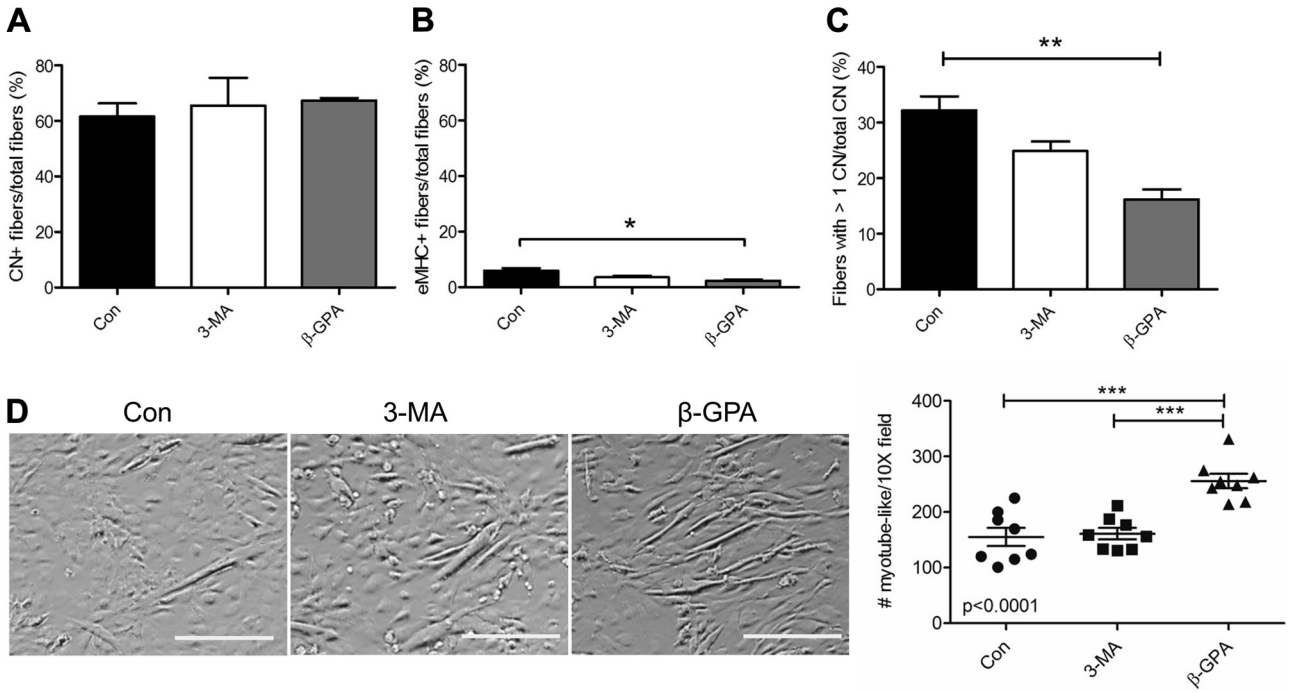

Fig. 5. Effect of 3-MA and β-GPA treatment on markers of muscle regeneration and myogenic differentiation in vivo and in vitro. *A* and *B*: quantification of regeneration in injured muscle demonstrates similar long-term regeneration by central nucleation (CN) and slightly reduced active regeneration [embryonic myosin heavy chain (eMHC)] in β-GPA-treated mice 14 days postinjury. *C*: number of fibers with >1 central nucleus as a proportion of the total number of regenerated fibers indicates a significant reduction in multi-central-nucleated fibers with β-GPA and a nonsignificant trend to reduction with 3-MA. *D*: C2C12 mouse myoblasts differentiated in low serum for 6 days with vehicle saline (Con), 1 mM 3-MA, or 1 mM β-GPA. Phase-contrast images with NucBlue nuclear staining (×10 objective) were analyzed for cells with myotube-like morphology. Each data point is the average of three ×10 images from a single well. Experiment was repeated 4 times, with 2 wells per condition for each experiment. Scale bar = 50 μm. *Statistically different from Con ($P < 0.05$). **Statistically different from Con ($P < 0.01$). ***Statistically different from β-GPA ($P < 0.001$).

injured than uninjured muscle independent of treatment ($P = 0.012$).

DISCUSSION

The mitochondrial network is a dynamic system essential for energy balance and redox homeostasis, and it may have an emerging role in regeneration of skeletal muscle and satellite cells. Because the mitochondrial network can be damaged with muscle injury (9, 28), there is sufficient need to investigate the mechanisms of mitochondrial regeneration. However, mitochondrial regeneration remains a relatively underinvestigated area of muscle repair. We sought to investigate the contribution of autophagy to mitochondrial regeneration during muscle repair. Our data indicate a robust induction of autophagy during muscle regeneration (Figs. 6 and 7), and we show that a broad-acting autophagy inhibitor negatively affects functional regeneration of skeletal muscle, in terms of both muscle strength and mitochondrial enzyme activity (Figs. 2 and 3). We show a near-complete recovery of muscle strength and mitochondrial enzyme activity in muscle with enhanced mitochondrial content (i.e., β-GPA-treated mice) by 14 days postinjury (Fig. 3), which demonstrates that β-GPA may positively influence muscle repair. We posit that the regeneration process is facilitated in part by autophagy, and we discuss below the broader impacts and limitations of our findings.

The recovery of muscle strength is the most functionally relevant marker of successful muscle regeneration (30). We decided to assess the relative success of muscle regeneration at 14 days postinjury based on the following rationale: *1*) satellite cell contribution to muscle regeneration, specifically differentiation and fusion, is largely complete by 14 days postinjury, and *2*) others have reported that markers of mitochondrial biogenesis have returned to baseline by 14 days postinjury. Therefore, in our minds, 14 days postinjury represents a critical transition period between muscle regeneration and muscle remodeling, when newly synthesized proteins are being utilized to repair or rebuild damaged organelles (i.e., mitochondria). Importantly, 3-MA-treated mice showed a substantial lack of recovery of muscle strength, in stark contrast to β-GPA-treated mice (Fig. 2), and this finding is not completely explained by differences in myogenic differentiation (Fig. 5). The functional deficit in injured muscle from 3-MA-treated mice may instead reflect an important role for the mitochondria during muscle repair, i.e., to meet the energy demands of muscle regeneration. The muscle contractions used to assess strength at 14 days postinjury were not aerobically demanding (i.e., 200-ms duration with 45 s between contractions); therefore, the mitochondrial dysfunction in injured 3-MA muscle (Fig. 3) is unlikely to directly contribute to the observed muscle weakness (Fig. 2). Instead, the dysfunctional mitochondria may limit aspects of late-stage satellite cell-mediated regeneration and/or remodeling. For instance, significant shifts have been reported in C2C12 myoblasts during differentiation to a predominantly oxidative metabolism in vitro (17), and inhibition of mitochondrial biogenesis during muscle regeneration negatively affected the recovery of fiber cross-sectional

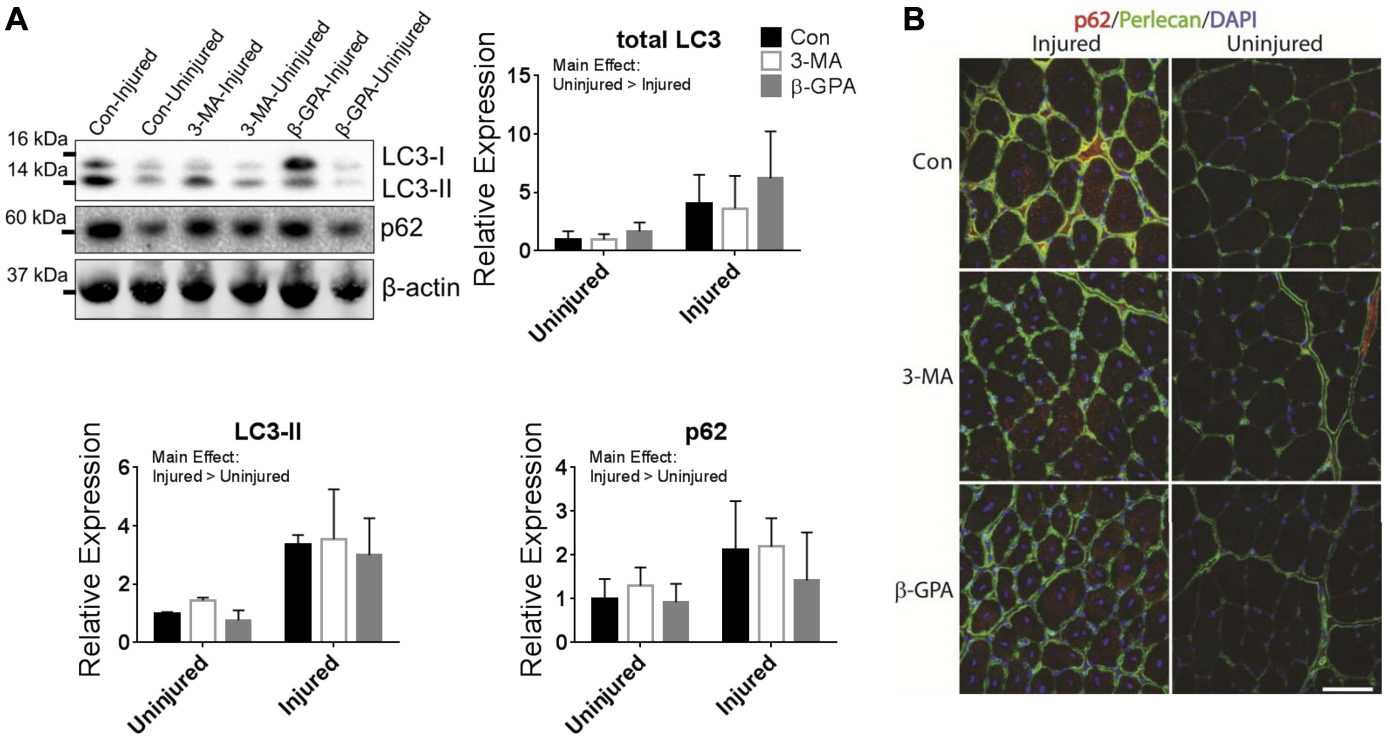

Fig. 6. Effect of treatments and injury on markers of autophagosome assembly and autophagy flux. *A*: immunoblot images and quantitative and statistical analysis (n = 6–8/group) of microtubule-associated protein 1A/1B-light chain 3 (LC3-I and LC3-II) and nucleoporin p62 (p62). β-Actin was probed as loading control. *B*: tibialis anterior muscle sections from Con and 3-MA- and β-GPA-treated mice were immunostained with anti-p62 and anti-perlecan to detect p62-positive puncta. 4′,6-Diamidino-2-phenylindole-stained nuclei are blue. Scale bar = 200 μm.

area at 10 days postinjury (28). It stands to reason then that mitochondrial function and dysfunction in injured muscle may play an important role in the success of muscle regeneration, which is supported by our use of β-GPA to enhance oxidative capacity and our finding that this treatment improved the functional recovery of muscle strength and mitochondrial enzyme activity (Figs. 2 and 3).

Analysis of the mitochondrial network during the early phases of muscle regeneration following myotoxic injury, i.e., within the first 10 days, shows several mitochondrial functional deficits and, not surprisingly, structural abnormalities as well (9, 28). However, the removal and rebuilding of the mitochondrial network following many muscle injuries have been a relatively overlooked aspect of muscle recovery in general, and it is worth speculating that the accumulation of dysfunctional mitochondria after several rounds of injury with impaired remodeling could lead to satellite cell dysfunction. Several studies have suggested that there is an accumulation of damaged mitochondria in skeletal muscle with age (7) and that altered autophagy signaling can contribute to the age-related mitochondrial dysfunction (31, 32). Our current study implemented the chronic use of a broad-acting autophagy inhibitor to recapitulate disease models with defective autophagy but without the co-morbidities. While 3-MA and other autophagy inhibitors are used in standard practice to compare rates of protein degradation with and without sufficient autophagy, these inhibitors are not without their limitations. 3-MA and other phosphatidylinositol inhibitors are broad-acting and, therefore, can have nonspecific effects and, indeed, have been shown to negatively impact other protein degradation processes (21). Nevertheless, 3-MA-treated muscles did show signs of impaired mitochondrial function (i.e., reduced SDH and β-HAD activities) (Fig. 3). It is reasonable that an accumulation of dysfunctional mitochondria during chronic 3-MA treatment contributed to impaired muscle regeneration. For example, 3 wk of a high-fat diet, which induces mitochondrial dysfunction (3), impaired muscle regeneration in otherwise healthy mice (33). A direct link between mitochondrial dysfunction and satellite function has yet to be established, but it is worth considering therapeutic modalities that could potentially enhance mitochondrial function to improve aforementioned diseased conditions (e.g., aging and obesity). Our work suggests that β-GPA treatment may have important clinical applications as a dietary intervention to improve maintenance of the mitochondria and remodeling during muscle regeneration.

β-GPA is a creatine analog that hinders the ATP-phosphocreatine system, thereby promoting mitochondrial biogenesis potentially through an AMPK-mediated signaling pathway (8, 23). While β-GPA is designated safe for human consumption, its effective dose and acute/chronic effects have not been widely investigated, potentially for several reasons. *1*) β-GPA-treated mice are reported to have greater mitochondrial enzyme activity (22), but the effective dose (1–2% of food intake by weight) and cost may in part contribute to a lack of scalability to human studies. *2*) Side effects of β-GPA treatment, i.e., decrements in body mass and muscle strength (Fig. 1) (22), have been reported and are potentially disadvantageous for populations in which the mitochondrial benefit of β-GPA is needed (e.g., the elderly). However, β-GPA may be a potential dietary supplement to bolster mitochondrial capacity in individuals who cannot participate in aerobic exercise or as a

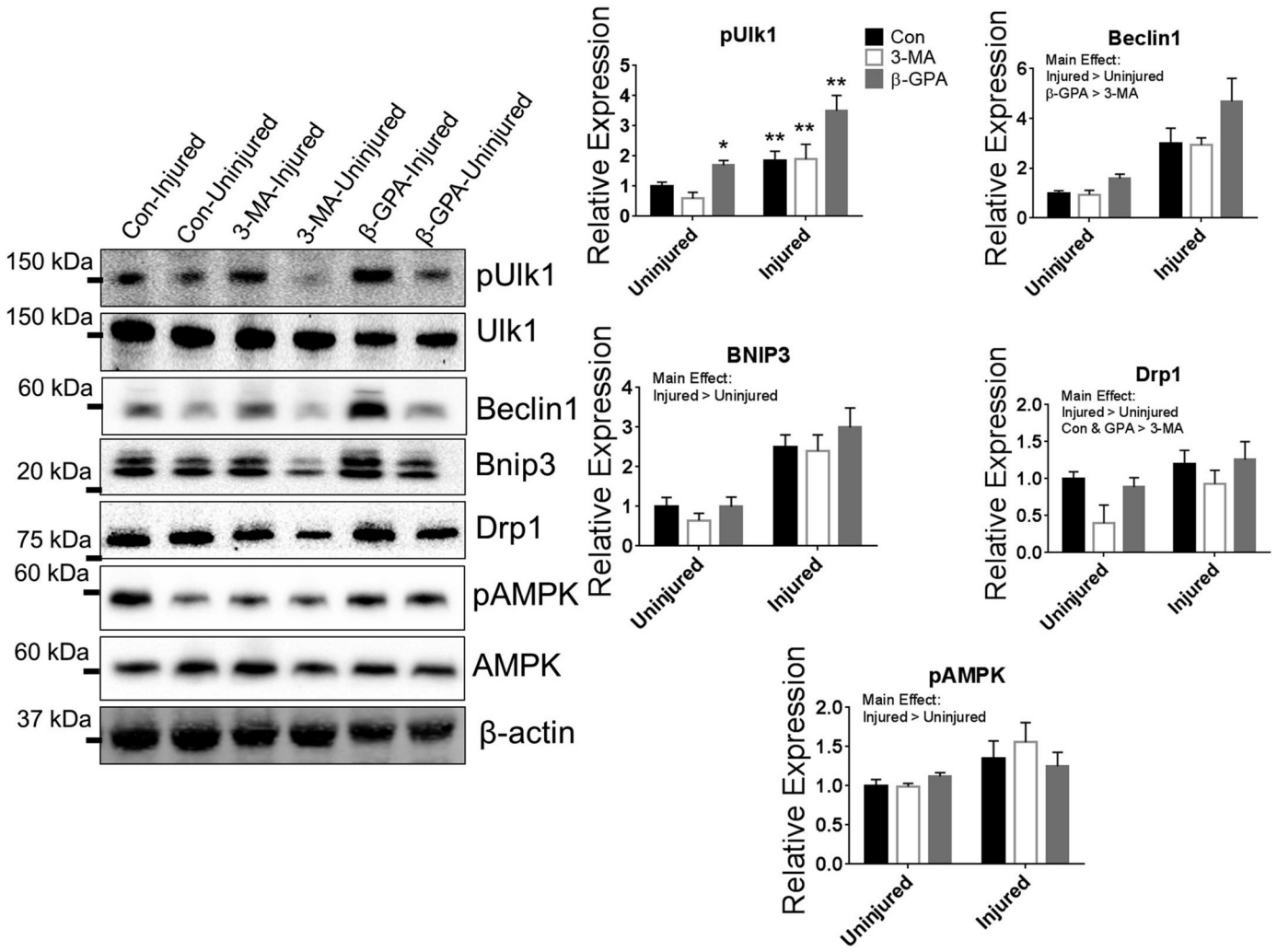

Fig. 7. Effect of treatments and injury on autophagy-related protein content. Immunoblot images and quantitative and statistical analysis (n = 6–8/group) of phosphorylated (Ser^{555}) Unc-51-like autophagy-activating kinase 1 (pUlk1), total Ulk1, Beclin1, Bnip3, dynamin-related protein 1 (Drp1), phosphorylated 5′-AMP-activated protein kinase (pAMPK), and total AMPK. β-Actin was probed as loading control. *Significantly different from 3-MA ($P < 0.05$). **Significantly greater than contralateral uninjured muscle within each group ($P < 0.05$).

means to augment beneficial exercise-training adaptations. We used β-GPA to manipulate the mitochondrial network in a way that contrasted autophagy inhibition with 3-MA. In line with reported effects of β-GPA, β-GPA-treated mice had greater fatigue resistance and mitochondrial enzyme activity in uninjured muscle. Interestingly, beyond the previously discussed finding of greater recovery of muscle strength and mitochondrial enzyme activity, β-GPA-treated mice also demonstrated a greater basal level of phosphorylated Ulk1, the autophagy-related protein associated with induction of mitochondrial autophagy. This finding may simply reflect the possibility that the level of basal autophagy may be related to oxidative capacity in skeletal muscle (18). We believe that these observations warrant more investigation into the role of β-GPA in mitochondrial maintenance.

The maintenance of the mitochondrial network involves the fusion of newly synthesized mitochondria following mitochondrial biogenesis balanced against the fission of damaged mitochondria to be degraded by autophagy (7). We observed a fairly robust autophagy response to muscle injury even 14 days after injury (Figs. 6 and 7). Most interesting were the data supporting the specific degradation of mitochondria, also known as mitophagy, which included greater activation of Ulk1 and greater Bnip3 and Drp1 protein content in injured muscle. While necrotic processes associated with inflammatory cell accumulation after muscle damage may be sufficient to degrade damaged mitochondria, this work supports at least a role for autophagy during the regeneration process, and autophagy may represent a target for enhancing regeneration when inflammatory processes are compromised (e.g., in aging). Our data suggest a disconnect between mitochondrial protein content (Fig. 4; no statistical difference between Con and 3-MA-treated mice) and enzyme activity (Fig. 3; statistical differences between Con and 3-MA-treated mice), suggesting that damaged/dysfunctional mitochondrial proteins in 3-MA-treated mice were not being properly degraded during the regeneration and remodeling processes following muscle injury.

In conclusion, there is an autophagy response to severe muscle damage that is detectable at 14 days postinjury.

Chronic and continuous treatment with a broad-acting autophagy inhibitor impaired functional muscle regeneration and mitochondrial remodeling after injury, suggesting that successful autophagy after muscle injury is important for muscle repair. In particular, mitochondrial enzyme activity, but not mitochondrial protein content, was negatively affected by autophagy inhibition in 3-MA-treated mice during muscle regeneration. This coincided with less recovery of preinjury muscle strength in 3-MA-treated mice, in stark contrast to the recovery of muscle strength in β-GPA-treated mice, which also demonstrated a near-complete recovery of mitochondrial enzyme activity. We posit that mitochondrial function plays a minor, albeit significant, role in muscle regeneration and that a link between mitochondrial maintenance and autophagy during muscle repair should be further explored.

ACKNOWLEDGMENTS

The authors thank Alexandra Flemington (University of Georgia) for contributions to this project.

DISCLOSURES

No conflicts of interest, financial or otherwise, are declared by the authors.

AUTHOR CONTRIBUTIONS

A.S.N., W.M.S., M.A., J.L., K.B.P., S.J.F., A.M.B., and J.A.C. performed the experiments; A.S.N., W.M.S., M.A., J.L., K.B.P., S.J.F., A.M.B., G.L.W., and J.A.C. analyzed the data; A.S.N., W.M.S., J.L., K.B.P., A.M.B., G.L.W., and J.A.C. interpreted the results of the experiments; A.S.N., W.M.S., and J.A.C. drafted the manuscript; A.S.N., W.M.S., M.A., J.L., K.B.P., S.J.F., A.M.B., G.L.W., and J.A.C. edited and revised the manuscript; A.S.N., W.M.S., M.A., J.L., K.B.P., S.J.F., A.M.B., G.L.W., and J.A.C. approved the final version of the manuscript; A.M.B., G.L.W., and J.A.C. developed the concept and designed the research; A.M.B. and J.A.C. prepared the figures.

REFERENCES

1. **Band M, Joel A, Hernandez A, Avivi A.** Hypoxia-induced BNIP3 expression and mitophagy: in vivo comparison of the rat and the hypoxia-tolerant mole rat, *Spalax ehrenbergi*. *FASEB J* 23: 2327–2335, 2009.
2. **Beedle AM, Turner AJ, Saito Y, Lueck JD, Foltz SJ, Fortunato MJ, Nienaber PM, Campbell KP.** Mouse fukutin deletion impairs dystroglycan processing and recapitulates muscular dystrophy. *J Clin Invest* 122: 3330–3342, 2012.
3. **Bonnard C, Durand A, Peyrol S, Chanseaume E, Chauvin MA, Morio B, Vidal H, Rieusset J.** Mitochondrial dysfunction results from oxidative stress in the skeletal muscle of diet-induced insulin-resistant mice. *J Clin Invest* 118: 789–800, 2008.
4. **Call JA, Chain KH, Martin KS, Lira VA, Okutsu M, Zhang M, Yan Z.** Enhanced skeletal muscle expression of extracellular superoxide dismutase mitigates streptozotocin-induced diabetic cardiomyopathy by reducing oxidative stress and aberrant cell signaling. *Circ Heart Fail* 8: 188–197, 2015.
5. **Call JA, Voelker KA, Wolff AV, McMillan RP, Evans NP, Hulver MW, Talmadge RJ, Grange RW.** Endurance capacity in maturing *mdx* mice is markedly enhanced by combined voluntary wheel running and green tea extract. *J Appl Physiol* 105: 923–932, 2008.
6. **Call JA, Warren GL, Verma M, Lowe DA.** Acute failure of action potential conduction in *mdx* muscle reveals new mechanism of contraction-induced force loss. *J Physiol* 591: 3765–3776, 2013.
7. **Calvani R, Joseph AM, Adhihetty PJ, Miccheli A, Bossola M, Leeuwenburgh C, Bernabei R, Marzetti E.** Mitochondrial pathways in sarcopenia of aging and disuse muscle atrophy. *Biol Chem* 394: 393–414, 2013.
8. **Chaturvedi RK, Adhihetty P, Shukla S, Hennessy T, Calingasan N, Yang L, Starkov A, Kiaei M, Cannella M, Sassone J, Ciammola A, Squitieri F, Beal MF.** Impaired PGC-1α function in muscle in Huntington's disease. *Hum Mol Genet* 18: 3048–3065, 2009.
9. **Duguez S, Feasson L, Denis C, Freyssenet D.** Mitochondrial biogenesis during skeletal muscle regeneration. *Am J Physiol Endocrinol Metab* 282: E802–E809, 2002.
10. **Fortunato MJ, Ball CE, Hollinger K, Patel NB, Modi JN, Rajasekaran V, Nonneman DJ, Ross JW, Kennedy EJ, Selsby JT, Beedle AM.** Development of rabbit monoclonal antibodies for detection of α-dystroglycan in normal and dystrophic tissue. *PLos One* 9: e97567, 2014.
11. **Gianni P, Jan KJ, Douglas MJ, Stuart PM, Tarnopolsky MA.** Oxidative stress and the mitochondrial theory of aging in human skeletal muscle. *Exp Gerontol* 39: 1391–1400, 2004.
12. **Hamai N, Nakamura M, Asano A.** Inhibition of mitochondrial protein synthesis impaired C2C12 myoblast differentiation. *Cell Struct Funct* 22: 421–431, 1997.
13. **He C, Bassik MC, Moresi V, Sun K, Wei Y, Zou Z, An Z, Loh J, Fisher J, Sun Q, Korsmeyer S, Packer M, May HI, Hill JA, Virgin HW, Gilpin C, Xiao G, Bassel-Duby R, Scherer PE, Levine B.** Exercise-induced BCL2-regulated autophagy is required for muscle glucose homeostasis. *Nature* 481: 511–515, 2012.
14. **Hochreiter-Hufford AE, Lee CS, Kinchen JM, Sokolowski JD, Arandjelovic S, Call JA, Klibanov AL, Yan Z, Mandell JW, Ravichandran KS.** Phosphatidylserine receptor BAI1 and apoptotic cells as new promoters of myoblast fusion. *Nature* 497: 263–267, 2013.
15. **Huard J, Li Y, Fu FH.** Muscle injuries and repair: current trends in research. *J Bone Joint Surg Am* 84A: 822–832, 2002.
16. **Landisch RM, Kosir AM, Nelson SA, Baltgalvis KA, Lowe DA.** Adaptive and nonadaptive responses to voluntary wheel running by *mdx* mice. *Muscle Nerve* 38: 1290–1303, 2008.
17. **Leary SC, Battersby BJ, Hansford RG, Moyes CD.** Interactions between bioenergetics and mitochondrial biogenesis. *Biochim Biophys Acta* 1365: 522–530, 1998.
18. **Lira VA, Okutsu M, Zhang M, Greene NP, Laker RC, Breen DS, Hoehn KL, Yan Z.** Autophagy is required for exercise training-induced skeletal muscle adaptation and improvement of physical performance. *FASEB J* 27: 4184–4193, 2013.
19. **Masiero E, Sandri M.** Autophagy inhibition induces atrophy and myopathy in adult skeletal muscles. *Autophagy* 6: 307–309, 2010.
20. **Mizushima N, Levine B, Cuervo AM, Klionsky DJ.** Autophagy fights disease through cellular self-digestion. *Nature* 451: 1069–1075, 2008.
21. **Mizushima N, Yamamoto A, Hatano M, Kobayashi Y, Kabeya Y, Suzuki K, Tokuhisa T, Ohsumi Y, Yoshimori T.** Dissection of autophagosome formation using Apg5-deficient mouse embryonic stem cells. *J Cell Biol* 152: 657–668, 2001.
22. **Oudman I, Clark JF, Brewster LM.** The effect of the creatine analogue β-guanidinopropionic acid on energy metabolism: a systematic review. *PLos One* 8: e52879, 2013.
23. **Pandke KE, Mullen KL, Snook LA, Bonen A, Dyck DJ.** Decreasing intramuscular phosphagen content simultaneously increases plasma membrane FAT/CD36 and GLUT4 transporter abundance. *Am J Physiol Regul Integr Comp Physiol* 295: R806–R813, 2008.
24. **Pauly M, Daussin F, Burelle Y, Li T, Godin R, Fauconnier J, Koechlin-Ramonatxo C, Hugon G, Lacampagne A, Coisy-Quivy M, Liang F, Hussain S, Matecki S, Petrof BJ.** AMPK activation stimulates autophagy and ameliorates muscular dystrophy in the *mdx* mouse diaphragm. *Am J Pathol* 181: 583–592, 2012.
25. **Ryall JG.** Metabolic reprogramming as a novel regulator of skeletal muscle development and regeneration. *FEBS J* 280: 4004–4013, 2013.
26. **Sandri M.** Autophagy in health and disease. 3. Involvement of autophagy in muscle atrophy. *Am J Physiol Cell Physiol* 298: C1291–C1297, 2010.
27. **Selsby JT, Morine KJ, Pendrak K, Barton ER, Sweeney HL.** Rescue of dystrophic skeletal muscle by PGC-1α involves a fast to slow fiber type shift in the *mdx* mouse. *PLos One* 7: e30063, 2012.
28. **Wagatsuma A, Kotake N, Yamada S.** Muscle regeneration occurs to coincide with mitochondrial biogenesis. *Mol Cell Biochem* 349: 139–147, 2011.
29. **Wang H, Hiatt WR, Barstow TJ, Brass EP.** Relationships between muscle mitochondrial DNA content, mitochondrial enzyme activity and oxidative capacity in man: alterations with disease. *Eur J Appl Physiol Occup Physiol* 80: 22–27, 1999.
30. **Warren GL, Lowe DA, Armstrong RB.** Measurement tools used in the study of eccentric contraction-induced injury. *Sports Med* 27: 43–59, 1999.
31. **Wohlgemuth SE, Lees HA, Marzetti E, Manini TM, Aranda JM, Daniels MJ, Pahor M, Perri MG, Leeuwenburgh C, Anton SD.** An exploratory analysis of the effects of a weight loss plus exercise program on cellular quality control mechanisms in older overweight women. *Rejuvenation Res* 14: 315–324, 2011.

32. **Wohlgemuth SE, Seo AY, Marzetti E, Lees HA, Leeuwenburgh C.** Skeletal muscle autophagy and apoptosis during aging: effects of calorie restriction and life-long exercise. *Exp Gerontol* 45: 138–148, 2010.
33. **Woo M, Isganaitis E, Cerletti M, Fitzpatrick C, Wagers AJ, Jimenez-Chillaron J, Patti ME.** Early life nutrition modulates muscle stem cell number: implications for muscle mass and repair. *Stem Cells Dev* 20: 1763–1769, 2011.
34. **Wu Z, Puigserver P, Andersson U, Zhang C, Adelmant G, Mootha V, Troy A, Cinti S, Lowell B, Scarpulla RC, Spiegelman BM.** Mechanisms controlling mitochondrial biogenesis and respiration through the thermogenic coactivator PGC-1. *Cell* 98: 115–124, 1999.
35. **Zhang J, Ney PA.** Role of BNIP3 and NIX in cell death, autophagy, and mitophagy. *Cell Death Differ* 16: 939–946, 2009.